Motion from Projections

Peyman Milanfar
SRI International
333 Ravenswood Ave. MS 404-69
Menlo Park, CA 94025
Phone: (415) 859-3745
Fax: (415) 859-6259
e-mail: milanfar@unix.sri.com

Abstract

Aside from computed tomography, the Radon (projection) transform has proven, in the recent past, to be quite a useful tool in a variety of image processing and computer vision tasks. In many classical and more recent applications, it is increasingly useful and informative to understand, and model, how certain properties of the image are mapped into the projection domain via the Radon transform. Understanding such relationships often results in the development of better and faster algorithms for image understanding, processing, or reconstruction.

In this paper, we will discuss generalizations of the shift property of the Radon transform and apply these results to the study of how motion in the image domain is manifested in the projection domain. We further develop various properties of the apparent projected motion, and study the case of affine motion in some depth. We also present illustrative examples and speculate on possible applications.

I. Introduction

The study of the Radon transform is at the heart of computed tomography as a diagnostic tool. More recently, however, this transform has been found to be increasingly useful as a general image analysis tool [1], [2]. Many of its fundamental properties have been exploited to study diverse problems including time-frequency analysis [3], feature extraction [4], [1], and motion estimation [5], [6].

A particularly useful application of the Radon transform has been in translational motion estimation from a video sequence [6], [5], and the related problem of image registration [2]. In particular, the shift property of the Radon transform shows that translational motion in the image domain results in translational motion in the projection domain. Namely, the Radon transform of $f(x - x_0, y - y_0)$ is simply given by $g(p - x_0 \cos\theta - y_0 \sin\theta, \theta)$, where $g(p, \theta) = \mathcal{R}_\theta[f]$ is the projection of $f(x, y)$ at angle θ. Hence, for instance, a two-dimensional motion estimation problem can essentially be decomposed into a pair of independent one-dimensional motion estimation problems, hence resulting in significant computational savings. To the extent that the underlying motion can be adequately modeled as translational, this shifting property of the Radon transform is also useful in motion compensation for computed tomography where projections are obtained while the subject (say a medical patient during a CAT scan, or a body of water during ocean acoustic tomography) is in motion. In such cases, it is necessary to "correct" the projections, before a reasonable reconstruction can be effected.

A revised and condensed version of this paper appeared in IEEE Trans. on Image Proc. vol.8, no. 9, pp. 1276-1281, Sept. 1999

Having considered translational motion, one might naturally wonder what happens in the projection domain if the motion in the image domain is *not* a simple displacement. As an example, respiratory motion during CAT scans can be modeled as a combination of expansion (magnification) and displacement [7]. The shifting property of the Radon transform is no longer sufficient to describe the effect of general motion in the image on the projections. Hence a generalization is clearly needed. In this paper, we will discuss such generalizations and study their implications and properties. In particular, we will study the case of affine motion in some detail and provide some illustrative examples. We will furthermore speculate on future directions of research and applications.

II. Preliminaries

We begin by defining the Radon transform and presenting some of its most fundamental properties that will be exploited later in this paper. The Radon transform maps a function $f(x, y)$ defined over a region D of the plane to a function $g(t, \theta)$ as follows:

$$g(p, \theta) = \mathcal{R}_\theta [f] = \iint_D f(x, y)\delta(p - x\cos(\theta) - y\sin(\theta))\, dx\, dy. \tag{1}$$

Namely, $g(p, \theta)$ is the integral of f over a line at angle $\theta + (\pi/2)$ with the x-axis, and a radial distance of p away from the origin. The above definition in two dimensions can be generalized so that if f is defined over an n-dimensional Euclidean space, then $g(p, w)$ will denote the integral of f over hyperplanes of dimension $n - 1$, where w denotes a direction vector at the origin and normal to the hyperplane.

A. Radon Transform Properties

We next state some elementary properties of the Radon transform without proof. The interested reader may find proofs in [8]. Though they are generally valid in n dimensions, for the sake of simplicity, we state these properties in two dimensions.

P 1: Linearity

$$\mathcal{R}_\theta [\alpha f + \beta h] = \alpha \mathcal{R}_\theta [f] + \beta \mathcal{R}_\theta [h] \tag{2}$$

P 2: Periodicity

For integer k,

$$g(p, \theta) = g(p, \theta + 2k\pi) \tag{3}$$

P 3: Symmetry

$$g(p, \theta) = g(-p, \theta + \pi) \tag{4}$$

P 4: Scaling

$$\mathcal{R}_\theta [f(\lambda x, \lambda y)] = \frac{1}{\lambda} g(\lambda p, \theta) \tag{5}$$

P 5: Inner-product

For any (square-integrable) function $H(p)$,

$$\int g(p,\theta)\; H(p)\; dp = \iint f(x,y) H(x\cos(\theta) + y\sin(\theta))\; dx\; dy. \tag{6}$$

In particular, the *Fourier-Slice Theorem*, relating the 1-D Fourier transform of g to the 2-D Fourier transform of f, is obtained by replacing $H(p)$ with a complex exponential. Furthermore, by letting $H(p) = p^k$, we obtain the moment property relating the moments of g to the moments of f:

$$\int g(p,\theta)\; p^k\; dp = \iint f(x,y)(x\cos(\theta) + y\sin(\theta))^k\; dx\; dy. \tag{7}$$

P 6: Shifting

If $v_0 = [v_{0x},\; v_{0y}]^T$ is a vector in the (x, y) plane,

$$\mathcal{R}_\theta\left[f(x - v_{0x}, y - v_{0y})\right] = g(p - v_0^T w(\theta), \theta), \tag{8}$$

where $w(\theta) = [\cos\theta,\; \sin\theta]^T$.

P 7: Transform of Derivatives

Let $L(\partial/\partial x, \partial/\partial y)$ denote a linear differential operator, and write the direction vector $w(\theta) = [w_1,\; w_2]^T$. We have

$$\mathcal{R}_\theta\left[L\; f\right] = L(w_1\partial/\partial p,\; w_2\partial/\partial p)\; g(p, w). \tag{9}$$

In particular, if L is a homogeneous polynomial of degree m with constant coefficients, then

$$\mathcal{R}_\theta\left[L\; f\right] = L(w)\frac{\partial^m g(p,w)}{\partial p^m}. \tag{10}$$

For instance, a useful corollary is

$$\mathcal{R}_\theta\left[v_0^T\; \nabla f\right] = v_0^T w\; \frac{\partial g(p,w)}{\partial p}. \tag{11}$$

P 8: Derivatives of the Transform

For integer k and l,

$$\frac{\partial^{k+l}\; g(p,w)}{\partial w_1^k\;\; \partial w_2^l} = \left(-\frac{\partial}{\partial p}\right)^{k+l} \mathcal{R}_\theta\left[x^k y^l f(x,y)\right], \tag{12}$$

where it must be kept in mind that when derivatives with respect to components of w are computed, the vector w is initially *not* considered a unit vector. The derivatives may later be evaluated for unit direction vectors such as $w(\theta) = [\cos\theta,\; \sin\theta]^T$.

P 9: Hermite Polynomials

Let $H_k(p)$ denote the k-th order Hermite polynomial defined by

$$e^{-p^2}\; H_k(p) = (-1)^k \left(\frac{\partial}{\partial p}\right)^k e^{-p^2}. \tag{13}$$

Then,

$$\mathcal{R}_\theta\left[H_k(x)H_l(y)e^{-x^2-y^2}\right] = \sqrt{\pi}\frac{w_1^k w_2^k}{\sqrt{w_1^2+w_2^2}}(-1)^{k+l}\left(\frac{\partial}{\partial p}\right)^{k+l}\exp\left(-\frac{p^2}{w_1^2+w_2^2}\right) \tag{14}$$

or if w is the standard unit direction vector, $w = [\cos\theta,\ \sin\theta]^T$

$$\mathcal{R}_\theta\left[H_k(x)H_l(y)e^{-x^2-y^2}\right] = \sqrt{\pi}\,(\cos\theta)^k\,(\sin\theta)^l\,e^{-p^2}H_{k+l}(p) \tag{15}$$

III. Motion in the Projection Domain

Given the properties listed above, we are now in a position to study motion in the projection domain. Consider an image sequence $f(x,y,t)$, which evolves in time according to the spatially varying motion vector field $v(x,y) = [v_1(x,y),\ v_2(x,y)]^T$. Also, consider its corresponding Radon transform sequence $g(p,\theta,t)$, obtained by computing the Radon transform of f for every fixed t. What we aim to show in this section is that, subject to some conditions, the displaced image $f(x+v_1\Delta t, y+v_2\Delta t, t+\Delta t)$ has a corresponding Radon transform which we can denote by $g(p+u\Delta t,\theta,t+\Delta t)$, where $u = u(p,\theta,t)$ is the (scalar) motion field induced in the projection domain by motion field v in the image domain. That is, we show that *locally*, the function u exists and is well defined, and that it adequately reflects the behavior of motion induced in the projection domain.

Let us compute, for a sufficiently small time increment Δt, a first order Taylor series expansion of f as follows:

$$f(x+v_1\Delta t, y+v_2\Delta t, t+\Delta t) \approx f(x,y,t) + v_1\frac{\partial f}{\partial x}\Delta t + v_2\frac{\partial f}{\partial y}\Delta t + \frac{\partial f}{\partial t}\Delta t \tag{16}$$

$$= f(x,y,t) + v^T\nabla f\ \Delta t + \frac{\partial f}{\partial t}\ \Delta t \tag{17}$$

Next, we consider the Radon transform applied to both sides of the above:

$$\mathcal{R}_\theta\left[f(x+v_1\Delta t, y+v_2\Delta t, t+\Delta t)\right] \approx \mathcal{R}_\theta\left[f(x,y,t) + v^T\nabla f\ \Delta t + \frac{\partial f}{\partial t}\ \Delta t\right] \tag{18}$$

$$= g(p,\theta,t) + \mathcal{R}_\theta\left[v^T\nabla f\right]\ \Delta t + \frac{\partial g(p,\theta,t)}{\partial t}\ \Delta t \tag{19}$$

Now *define* the function $u(p,\theta,t)$ by

$$u(p,\theta,t) = \frac{\mathcal{R}_\theta\left[v^T\nabla f(x,y,t)\right]}{\partial g(p,\theta,t)/\partial p}. \tag{20}$$

Clearly, this function is well-defined only when $\partial g(p,\theta,t)/\partial p \neq 0$, and when $f(x,y,t)$ is differentiable. We will discuss these requirements in more depth a bit later. For now, assuming that u is thus well-defined, if we replace its definition into (19), we have

$$\mathcal{R}_\theta\left[f(x+v_1\Delta t, y+v_2\Delta t, t+\Delta t)\right] \approx g(p,\theta,t) +\ u(p,\theta,t)\frac{\partial g(p,\theta,t)}{\partial p}\Delta t + \frac{\partial g(p,\theta,t)}{\partial t}\ \Delta t \tag{21}$$

The right-hand side of (21) now appears quite similar to a Taylor series expansion of $g(p,\theta,t)$. In fact, if $u(p,\theta,t)$ is replaced by dp/dt, we will have exactly the first-order Taylor series of g on the right-hand side. We can make this substitution only when the differential equation

$$\frac{dp}{dt} = u(p,\theta,t), \tag{22}$$

has a solution, for any fixed θ, over the support of g on the axis p. The existence and uniqueness theorem for first-order ordinary differential equations [9] states that a unique solution to (22) will exist when $u(p,\theta,t)$ is continuously differentiable (or C^1); that is, $\partial u/\partial p$ must exist and be continuous[1] on a compact subset of the p-axis. Referring to the definition of u in (20), we can see that if we require that the vector field v be C^1 and that f be C^2, then $\partial u/\partial p$ exists, it is continuous, and is given by

$$\begin{aligned} \frac{\partial u}{\partial p} &= \frac{\left(\partial \mathcal{R}_\theta[v^T\nabla f]/\partial p\right)(\partial g/\partial p) - (\partial^2 g/\partial p^2)\,\mathcal{R}_\theta[v^T\nabla f]}{(\partial g/\partial p)^2} & (23)\\ &= \frac{\mathcal{R}_\theta[w^T\nabla(v^T\nabla f)]\mathcal{R}_\theta[w^T\nabla f] - \mathcal{R}_\theta[\nabla^2 f]\mathcal{R}_\theta[v^T\nabla f]}{(\mathcal{R}_\theta[w^T\nabla f])^2}, & (24)\end{aligned}$$

where $\nabla^2 f$ denotes the Laplacian of f, and the last identity follows by invoking property **P7**. Note that, as before, we have assumed that $\partial g/\partial p \neq 0$. Therefore, taking both f and v to be defined over the same compact region of the plane (the image region), we have the following result.

Theorem 1 (Projected Motion) Consider the image sequence $f(x,y,t)$, assumed to be twice continuously differentiable (or C^2), which evolves according to the C^1 vector field $v(x,y)$. Then, for any θ, there exists a C^1 function $u(p,\theta,t)$ such that, to first order,

$$\mathcal{R}_\theta\left[f(x+v_1\Delta t, y+v_2\Delta t, t+\Delta t)\right] = g(p+u\Delta t,\theta,t+\Delta t), \tag{25}$$

for sufficiently small Δt. Furthermore, the function u is given by the identity

$$u(p,\theta,t)\frac{\partial g(p,\theta,t)}{\partial p} = \mathcal{R}_\theta\left[v^T\nabla f(x,y,t)\right] \tag{26}$$

whenever $\partial g/\partial p \neq 0$. We term this relationship the *differential* **Projected Motion Identity** (PMI). □

A straightforward corollary of the above result is that under the same assumptions, we have

$$\frac{dg}{dt} = \mathcal{R}_\theta\left[\frac{df}{dt}\right]. \tag{27}$$

That is, locally, the projection of the total derivative of f is the total derivative of the projection of f ($\mathcal{R}_\theta$ and the total derivative operation commute). An immediate consequence is that if the optical

[1] This will imply that u and $\partial u/\partial p$ are also bounded on the same interval.

flow brightness constraint $df/dt = 0$ is assumed to hold, then (27) implies that this constraint also holds in the projection domain: $dg/dt = 0$, with motion in this domain given by (26).

The PMI is in essence a natural generalization of the well-known shift property (**P6**) of the Radon transform. In particular, if the motion vector $v = v_0$ is spatially invariant, then property **P7** gives

$$\mathcal{R}_\theta \left[v_0^T \nabla f \right] = v_0^T w(\theta) \frac{\partial g}{\partial p}, \tag{28}$$

where $w(\theta) = [\cos(\theta), \sin(\theta)]^T$. Comparing the above identity to (26), we observe that for spatially invariant motion, $u = v_0^T w(\theta)$, as expected. Furthermore, it is worth noting that as with the shift property, the PMI generalization holds in any dimension. That is, if the Radon transform of a scalar function of n real variables is defined as its integrals over hyperplanes of dimension $n-1$, the arguments presented above would yield the same result except that v would be an n-dimensional vector field.

Several comments are in order. First, we note that u is time-varying even though the vector field v may not be so. This is simply due to the dependence of u on the gradient of the image, which varies with time. Another observation worth making is that by invoking the directional derivative property **P7**, we can rewrite $\partial g / \partial p$ in the image domain and express the PMI as follows:

$$u(p, \theta, t) \mathcal{R}_\theta \left[w^T \nabla f \right] = \mathcal{R}_\theta \left[v^T \nabla f \right]. \tag{29}$$

The insight we gain here is that u is expressible as the *ratio* of two projections. Namely, the projection of the directional derivative of the image parallel to v (sometimes called the *advective* derivative of f), and the directional derivative of the image parallel to the unit vector $w(\theta)$, when the latter projection is not zero. Intuitively, at points where $\mathcal{R}_\theta \left[w^T \nabla f \right]$ vanishes, there is no perceived motion in the projection taken at angle θ, and hence, as expected, u is not well defined. It is also interesting to note that in each direction of projection, the correspondence between the vector field v and the function u is not unique. Namely, for a given θ, both v and $v + v_\perp$ yield the same u if $v_\perp$ is such that $\mathcal{R}_\theta [v_\perp^T \nabla f] = 0$.

It is important to note that other forms of the PMI, based upon more restrictive global conservation assumptions, are also possible. Namely, Fitzpatrick [10] considers f and v both C^1, where f is to represent the density of some *conserved* quantity. That is

$$\frac{\partial f}{\partial t} + \operatorname{div}(fv) = 0, \tag{30}$$

which is the familiar continuity equation of fluid dynamics. Here we present a generalized rederivation of Fitzpatrick's expression for u using the Radon transform properties described earlier. Write

$$\frac{\partial f}{\partial t} + \operatorname{div}(fv) = \frac{\partial f}{\partial t} + \frac{\partial (f v_1)}{\partial x} + \frac{\partial (f v_2)}{\partial y} = 0, \tag{31}$$

Taking the Radon transform of both sides of (31), and applying property **P7** we have

$$\frac{\partial g}{\partial t} + \mathcal{R}_\theta\left[\frac{\partial(fv_1)}{\partial x}\right] + \mathcal{R}_\theta\left[\frac{\partial(fv_2)}{\partial y}\right] = \frac{\partial g}{\partial t} + w_1\frac{\partial}{\partial p}\mathcal{R}_\theta\left[fv_1\right] + w_2\frac{\partial}{\partial p}\mathcal{R}_\theta\left[fv_2\right] \quad (32)$$

$$= \frac{\partial g}{\partial t} + \frac{\partial}{\partial p}\mathcal{R}_\theta\left[f\, v^T w\right] = 0. \quad (33)$$

Now if we define

$$u_c(p,\theta,t)g(p,\theta,t) = \mathcal{R}_\theta\left[f\, v^T w\right], \quad (34)$$

whenever $g \neq 0$, and replace this definition into (33), we obtain a continuity equation for g:

$$\frac{\partial g}{\partial t} + \frac{\partial(u_c g)}{\partial p} = 0. \quad (35)$$

The identity (34) is the PMI implied by the conservation assumption (hence the subscript c on u). The existence and uniqueness of a solution to $dp/dt = u_c$ is discussed in [10] in some detail. The issue of whether (26) or (34) should be used in describing the nature of motion in the projection domain is a matter of which assumptions are most adequate in describing the application at hand. However, while the differential form of PMI makes slightly stronger smoothness assumptions on f, it is more generally applicable as it is not based on a global conservation assumption. In particular, let us distinguish the two cases by referring to (34) as the *integral* (or conservative) PMI, where as without this qualification, we will understand *differential* PMI to mean the version in (26). It is worthwhile to highlight some similarities and differences between these two concepts. Namely, both formulations require a C^1 vector field v; but while integral PMI assumes a C^1 image sequence, differential PMI is formulated for C^2 images[2]. On the other hand, differential PMI is a local result based upon a local series development, while the integral version of PMI relies on a global conservation assumption. Similar to the differential PMI, the integral PMI also implies a description of u as the *ratio* of two projection: $u_c\, \mathcal{R}_\theta[f] = \mathcal{R}_\theta[fv^T w]$. That is, u is the ratio of the projection of the *flux* (fv) in the direction of w, to the projection of f itself in the same direction. As we shall see next, u and u_c share many similar properties.

IV. Properties of Projected Motion

A number of interesting properties of projected motion can be derived directly from the properties of the Radon transform stated earlier. We will develop these properties based on both the differential version (26) of the PMI, and the integral version in (34).

A. The Fourier Slice Theorem (FST) for Projected Motion

The FST states that the 1-D Fourier transform of the projection g, at angle θ, of f is equal to a central slice, at angle θ, of the 2-D Fourier transform of f. If we take the 1-D Fourier transform (in

[2]Note that the to satisfy $f \in C^n$, it is sufficient to convolve any given image with a differentiable point-spread function n times.

the variable p) of both sides of the (26) for fixed θ, and apply the FST, we obtain

$$\begin{aligned} \mathcal{F}\left[u(p,\theta,t)\right] * \mathcal{F}\left[\partial g/\partial p\right] &= \mathcal{F}\left[\mathcal{R}_\theta\left[v^T \nabla f\right]\right] & (36) \\ U(\omega_p,\theta,t) * j\omega_p \mathcal{F}\left[g\right] &= \mathcal{F}\left[v^T \nabla f\right]_{\text{slice}\,\theta} & (37) \\ U(\omega_p,\theta,t) * j\omega_p G(\omega_p,\theta,t) &= \mathcal{F}\left[v^T \nabla f\right]_{\text{slice}\,\theta}, & (38) \end{aligned}$$

where $*$ denotes the (1-D) convolution operator. The above is a relationship between u and v in the spectral domain, in the spirit of the FST.

For the integral PMI, the corresponding result is

$$U_c(\omega_p,\theta,t) * G(\omega_p,\theta,t) = \mathcal{F}\left[f\ v^T w\right]_{\text{slice}\,\theta} \tag{39}$$

B. Linearity

The linearity of the Radon transform implies that the PMI (both integral and differential) is additive in the following sense. For a given image f, if u and u' are the projected motions resulting from the vector fields v and v' respectively, then the projected motion field resulting from $av + bv'$ is simply $au + bu'$, where a and b are arbitrary scalars.

In particular, if a given vector field v is decomposed according to Helmholtz's theorem [11] into its irrotational and solenoidal components as $v = v_I + v_S$, then it follows that the projected motion field u essentially has a decomposition of the same kind $u = u_I + u_S$. That is, Helmholtz's theorem projects into the Radon transform domain.

C. Periodicity

Property **P2** states that the Radon transform is periodic in the variable θ with period 2π. Applying this property to the either form of the PMI, we see that the projected motion is also periodic with the same period. Writing out the differential PMI,

$$h(p,\theta,t) = \mathcal{R}_\theta\left[v^T \nabla f\right] = u(p,\theta,t)\frac{\partial g(p,\theta,t)}{\partial p} \tag{40}$$

and invoking the periodicity of h, we can write

$$u(p,\theta+2k\pi)\frac{\partial g(p,\theta+2k\pi,t)}{\partial p} = u(p,\theta,t)\frac{\partial g(p,\theta,t)}{\partial p}. \tag{41}$$

But since g is also periodic, that is, $g(p,\theta+2k\pi,t) = g(p,\theta,t)$ for any integer k, we immediately get

$$u(p,\theta+2k\pi,t) = u(p,\theta,t) \tag{42}$$

whenever $\partial g/\partial p \neq 0$. A similar argument shows periodicity for u_c, with the same period.

D. Anti-Symmetry

The symmetry property **P3** can be used to show that u is *anti*-symmetric. Again, invoking the symmetry of h, we get

$$u(p,\theta,t)\frac{\partial g(p,\theta,t)}{\partial p} = u(-p,\theta+\pi,t)\frac{\partial g(-p,\theta+\pi,t)}{\partial(-p)}. \tag{43}$$

Now invoking the symmetry of g, we have

$$u(p,\theta,t)\frac{\partial g(p,\theta,t)}{\partial p} = -u(-p,\theta+\pi,t)\frac{\partial g(p,\theta,t)}{\partial p}, \tag{44}$$

which implies that

$$u(p,\theta,t) = -u(-p,\theta+\pi,t), \tag{45}$$

whenever $\partial g/\partial p \neq 0$.

The corresponding result for u_c is the same, and the result follows by noting that the right-had side of (34), due to the presence of the unit direction vector $w(\theta)$, is anti-symmetric.

E. Moments

The moment property **P5** of the Radon transform relates the k-th order moments of an image to those of its projections. Since the differential PMI shows that $v^T\nabla f$ and $u\ \partial g/\partial p$ are a Radon transform pair, we can apply the moment property to get (for fixed t):

$$\iint v^T\nabla f(x,y,t)\ \ (x\cos\theta + y\sin\theta)^k\ \ dx\ dy = \int p^k\ u(p,\theta,t)\ \frac{\partial g}{\partial p}\ dp. \tag{46}$$

In particular, for $k=0$, we get

$$\iint v^T\nabla f(x,y,t)\ dx\ dy = \int u(p,\theta,t)\ \frac{\partial g}{\partial p}dp. \tag{47}$$

In simple terms, this means that the integral of the advective derivative of f over the entire image is equal to the integral of the advective derivative of the projection g (taken in any direction). This is an intuitively pleasing result; namely, that projection conserves the average advective derivative[3] of f.

A somewhat different, but equally interesting conclusion is drawn from the integral PMI. Namely, a similar argument shows that

$$\iint f(x,y,t)\, v^T w\ \ (x\cos\theta + y\sin\theta)^k\ \ dx\ dy = \int p^k\ u_c(p,\theta,t)\ g\ dp. \tag{48}$$

In particular, for $k=0$, we get

$$\iint f(x,y,t)\, v^T w\ dx\ dy = \int u_c(p,\theta,t)\ g\ dp, \tag{49}$$

which simply means that the total flux of f in the direction of $w(\theta)$ is equal to the total flux in the projection g at angle θ; i.e. total flux in any direction is conserved by projection.

[3]Recall that projection also conserves the total mass of f.

V. Analysis of Affine Motion in the Projection Domain

Any motion field can be locally approximated (to first order) by affine motion. That is, we can consider the class of motions given by

$$v = v_0 + M \begin{bmatrix} x \\ y \end{bmatrix}, \qquad M = \begin{bmatrix} a & b \\ c & d \end{bmatrix}. \tag{50}$$

where v_0 is a fixed vector denoting translational motion.

An important reason for considering the class of affine motions is that they can be easily decomposed into rotational, divergent, and shearing components. That is, the matrix M can be written as follows:

$$M = \frac{a+d}{2}\begin{bmatrix} 1 & 0 \\ 0 & 1 \end{bmatrix} + \frac{c-b}{2}\begin{bmatrix} 0 & -1 \\ 1 & 0 \end{bmatrix} + \frac{a-d}{2}\begin{bmatrix} 1 & 0 \\ 0 & -1 \end{bmatrix} + \frac{b+c}{2}\begin{bmatrix} 0 & 1 \\ 1 & 0 \end{bmatrix}, \tag{51}$$

where the first term of the above sum corresponds to linear divergent motion represented by $[x,\ y]^T$; the second term corresponds to rotational motion represented by $[y,\ -x]^T$; and the final two terms correspond to shearing motions represented by $[x,\ -y]^T$ and $[y,\ x]^T$, respectively. Specifically, we have

$$\begin{aligned} \text{div}(v) &= a + d && (52)\\ \text{curl}(v) &= (c-b)\,[0,\ 0,\ 1]^T && (53)\\ \text{shear strength}(v) &= \sqrt{(a-d)^2 + (b+c)^2} && (54) \end{aligned}$$

Given this decomposition, the linearity property implied by either form of the PMI shows that the projection of any affine motion has a natural decomposition into translational, rotational, divergent, and shearing components. This indicates that it may be possible to probe each of these components separately in the projection domain and hence measure the corresponding component in the image domain.

In what follows we study how affine motion behaves in the projections domain. Specifically, since general image sequences of interest may not satisfy the conservation assumptions underlying the integral PMI, we carry out this study in the context of the more general differential PMI.

To see specifically how affine transformation behaves in the projection domain, let us consider warping an image $f(x, y)$ by such a transformation. Letting $f(x, y) = f(x, y, 0)$, if we compute the derivative of both sides of the differential PMI with respect to p and invoke properties **P1** and **P7**, we get

$$\begin{aligned} \frac{\partial}{\partial p}\left(u\,\frac{\partial g}{\partial p}\right) &= \frac{\partial}{\partial p}\left(\mathcal{R}_\theta\left[(ax+by)\frac{\partial f}{\partial x} + (cx+dy)\frac{\partial f}{\partial y}\right] + \mathcal{R}_\theta\left[v_0^T \nabla f\right]\right) && (55)\\ &= \frac{\partial}{\partial p}\mathcal{R}_\theta\left[x(a\frac{\partial f}{\partial x} + c\frac{\partial f}{\partial y})\right] + \frac{\partial}{\partial p}\mathcal{R}_\theta\left[y(b\frac{\partial f}{\partial x} + d\frac{\partial f}{\partial y})\right] + \frac{\partial}{\partial p}\left(v_0^T w \frac{\partial g}{\partial p}\right). && (56) \end{aligned}$$

Writing the direction vector $w = [w_1,\ w_2]^T$ and using property **P8** we can rewrite (56) as follows:

$$
\begin{aligned}
\frac{\partial}{\partial p}\left(u\,\frac{\partial g}{\partial p}\right) &= -\frac{\partial}{w_1}\mathcal{R}_\theta\left[a\frac{\partial f}{\partial x}+c\frac{\partial f}{\partial y}\right]-\frac{\partial}{w_2}\mathcal{R}_\theta\left[b\frac{\partial f}{\partial x}+d\frac{\partial f}{\partial y}\right]+\frac{\partial}{\partial p}\left(v_0^T w\frac{\partial g}{\partial p}\right) && (57)\\
&= -\frac{\partial}{w_1}\left[(aw_1+cw_2)\frac{\partial g}{\partial p}\right]-\frac{\partial}{w_2}\left[(bw_1+dw_2)\frac{\partial g}{\partial p}\right]+\frac{\partial}{\partial p}\left(v_0^T w\frac{\partial g}{\partial p}\right) && (58)\\
&= -\frac{\partial}{\partial p}\left[\frac{\partial}{w_1}(aw_1+cw_2)g+\frac{\partial}{w_2}(bw_1+dw_2)g-v_0^T w\frac{\partial g}{\partial p}\right] && (59)\\
&= -\frac{\partial}{\partial p}\left(\mathrm{tr}(M)g+w^T M\begin{bmatrix}\partial g/\partial w_1\\ \partial g/\partial w_2\end{bmatrix}-v_0^T w\frac{\partial g}{\partial p}\right). && (60)
\end{aligned}
$$

It is important to remark here that, as pointed out in [8] (p. 91), when derivatives with respect to the components of w are taken, the vector w is not considered as a unit vector initially. The derivative expression is first computed and then evaluated at $w = [\cos\theta,\ \sin\theta]^T$.

Integrating both sides of (60) with respect to p we get

$$\left(u - v_0^T w\right)\,\frac{\partial g}{\partial p} + \mathrm{tr}(M)g + w^T M\left[\partial g/\partial w_1,\ \partial g/\partial w_2\right]^T = \epsilon, \tag{61}$$

The indeterminate constant ϵ is the same for any choice of v_0, M and f. In fact, we can show that ϵ must necessarily be zero by letting $f = 0$. The case below, however, is more instructive:

$$
\begin{aligned}
f(x,y,0) &= \exp(-x^2-y^2), && (62)\\
v_0 &= \begin{bmatrix}0 & 0\end{bmatrix}^T, && (63)\\
M &= \begin{bmatrix}1 & 0\\ 0 & 1\end{bmatrix}. && (64)
\end{aligned}
$$

This yields

$$
\begin{aligned}
g(p,w,0) &= \sqrt{\pi}\left(w_1^2+w_2^2\right)^{-1/2}\exp\left[\frac{-p^2}{w_1^2+w_2^2}\right] && (65)\\
\left.\frac{\partial g}{\partial w_1}\right|_{|w|=1} &= \sqrt{\pi}\cos(\theta)(2p^2-1)e^{-p^2} && (66)\\
\left.\frac{\partial g}{\partial w_2}\right|_{|w|=1} &= \sqrt{\pi}\sin(\theta)(2p^2-1)e^{-p^2} && (67)
\end{aligned}
$$

From the example in Section VI-A, we have that the function u is given by $u(p,\theta,0) = p + (1/2p)$. Substituting the above quantities into (61) and simplifying we get $\epsilon = 0$. Hence, for affine motion in the projection domain, the following equation must be satisfied:

$$\left(u - v_0^T w\right)\,\frac{\partial g}{\partial p} + \mathrm{tr}(M)g + w^T M\left.\begin{bmatrix}\partial g/\partial w_1\\ \partial g/\partial w_2\end{bmatrix}\right|_{|w|=1} = 0. \tag{68}$$

As an aside, we can write the above more compactly as

$$\left(u - v_0^T w\right)\,\frac{\partial g}{\partial p} + \mathrm{div}\left.\left(gM^T w\right)\right|_{|w|=1} = 0, \tag{69}$$

where the divergence is computed with respect to the components w_1 and w_2 of the direction vector. It is also worth noting that as a consequence of the linearity property of the PMI, $u_m = u - v_0^T w$ is simply the *non-translational* part of the projected motion which satisfies the relationship in (69).

Much can be learned about the general structure of affine motion in the projection domain by considering the representation of the function f using Hermite polynomials. In particular, consider

$$f(x, y, 0) = \sum_{k,l} f_{kl} H_k(x) H_l(y) e^{-x^2-y^2}, \tag{70}$$

where $\{H_k(x)H_l(y);\ \ k, l = 0, 1, 2, \cdots\}$ is an orthogonal basis[4] with weight function $e^{-x^2-y^2}$, and we take the above sum to be uniformly convergent.

With this representation, and invoking property **P9**, the Radon transform of f is given by

$$g(p, w, 0) = \sqrt{\pi} \sum_{k,l} f_{kl} \frac{w_1^k w_2^k}{\sqrt{w_1^2 + w_2^2}} (-1)^{k+l} \left(\frac{\partial}{\partial p}\right)^{k+l} \exp\left(-\frac{p^2}{w_1^2 + w_2^2}\right), \tag{71}$$

which for $|w| = 1$ reduces to

$$g(p, w, 0) = \sqrt{\pi} \sum_{k,l} f_{kl}\, w_1^k\, w_2^l\, e^{-p^2}\, H_{k+l}(p). \tag{72}$$

The derivative of g with respect to p is given by

$$\frac{\partial g}{\partial p} = -\sqrt{\pi} \sum_{k,l} f_{kl}\, w_1^k\, w_2^l\, e^{-p^2}\, H_{k+l+1}(p). \tag{73}$$

Differentiating (71) with respect to the components w_1 and w_2 and then assuming $|w| = 1$ we get.

$$\frac{\partial g}{\partial w_1} = \sqrt{\pi}\, e^{-p^2} \sum_{k,l} f_{kl} w_1^{k-1} w_2^{l-1} \left[w_2(k - w_1^2) H_{k+l}(p) + 2w_1^2 w_2 X_{kl}(p)\right], \tag{74}$$

$$\frac{\partial g}{\partial w_2} = \sqrt{\pi}\, e^{-p^2} \sum_{k,l} f_{kl} w_1^{k-1} w_2^{l-1} \left[w_1(l - w_2^2) H_{k+l}(p) + 2w_2^2 w_1 X_{kl}(p)\right], \tag{75}$$

where

$$X_{kl}(p) = (-1)^{k+l} \left[\left(\frac{\partial}{\partial p}\right)^{k+l} p^2 + (-1)^{k+l} p^2 H_{k+l}(p)\right]. \tag{76}$$

For sufficiently large p, the function $X_{kl}(p)$ behaves asymptotically as

$$X_{kl}(p) \approx p^2 H_{k+l}(p). \tag{77}$$

Replacing the asymptotic expression for $X_{kl}(p)$ into (74) and (75) and simplifying gives

[4] While a shortcoming of this representation is that the basis functions $H_k(x)H_l(y)$ are not compactly supported when real images are, the inclusion of the exponential factor makes this representation somewhat more realistic for image processing.

$$\frac{\partial g}{\partial w_1} = \sqrt{\pi}\, e^{-p^2} \sum_{k,l} f_{kl} w_1^{k-1} w_2^l \,(k - w_1^2 + 2w_1^2 p^2) H_{k+l}(p) \tag{78}$$

$$\frac{\partial g}{\partial w_2} = \sqrt{\pi}\, e^{-p^2} \sum_{k,l} f_{kl} w_1^{k} w_2^{l-1} \,(l - w_2^2 + 2w_2^2 p^2) H_{k+l}(p). \tag{79}$$

The terms $(k - w_1^2 + 2w_1^2 p^2)$ and $(l - w_2^2 + 2w_2^2 p^2)$ may be further approximated by $2w_1^2 p^2$ and $2w_2^2 p^2$, respectively, when p is large. Finally, we obtain the rather simple expression

$$\left[\begin{array}{c} \partial g/\partial w_1 \\ \partial g/\partial w_2 \end{array} \right] \Bigg|_{|w|=1} = 2\sqrt{\pi} p^2 e^{-p^2} \sum_{k,l} f_{kl}\, w_1^k\, w_2^l\, H_{k+l}(p) \left[\begin{array}{c} w_1 \\ w_2 \end{array} \right] = 2p^2 g \left[\begin{array}{c} w_1 \\ w_2 \end{array} \right]. \tag{80}$$

Substituting this last expression into (68) and solving for u we obtain (assuming $\partial g/\partial p \neq 0$)

$$u \sim -\frac{g}{\partial g/\partial p} \left[\mathrm{tr}(M) + 2p^2 \left(w^T M w \right) \right] + v_0^T w \tag{81}$$

Referring to (72) and (73) we observe that

$$\frac{g}{\partial g/\partial p} \sim \frac{-H_{k+l}(p)}{H_{k+l+1}(p)} \approx \frac{-1}{2p}. \tag{82}$$

Finally, we obtain the following neat asymptotic expression for u:

$$u \sim v_0^T w + \left(w^T M w \right) p. \tag{83}$$

Expanding the quadratic form in M using (51), we may explicitly decompose u into its translational, divergent, rotational and shearing components as follows:

$$u(p,\theta,0) \approx v_{0x}\cos(\theta) + v_{0y}\sin(\theta) + \frac{a+d}{2} p + 0\, p + \left(\frac{a-d}{2}\cos(2\theta) + \frac{b+c}{2}\sin(2\theta) \right) p. \tag{84}$$

Note that in this asymptotic representation, the term corresponding to pure rotation (i.e., the coefficient corresponding to the curl strength $c - b$) is zero. In fact, what occurs is that the influence of any pure rotation in the image plane decays essentially as $1/p$ or faster in the projection domain and is therefore seen only near the center of rotation as we will show in Section VI-B.

It is interesting to note that for the particular choices $\theta = 0,\ \pi/2$, (83) becomes

$$u(p,0,0) \approx v_{0x} + a\, p, \tag{85}$$

$$u(p,\pi/2,0) \approx v_{0y} + d\, p. \tag{86}$$

Therefore, measuring u in these directions, we observe that two projections suffice to uniquely determine both v_0 and the diagonal elements of M. Furthermore, another projection at $\theta = \pi/4$ yields

$$u(p,\pi/4,0) \approx \frac{\sqrt{2}}{2}(v_{0x} + v_{0y}) + \frac{a+d}{2} p + \frac{b+c}{2} p. \tag{87}$$

Given the values of v_0, a, and d from the projections at 0 and $\pi/2$, we can find the sum $(b+c)$ by measuring $u(p, \pi/4, 0)$. Assuming that the curl strength $(c-b)$ is known a priori, the values of b and c are then determined uniquely. Hence, we have shown that away from $p=0$, three projections along with a priori knowledge of the curl suffice to determine uniquely any affine transformation v.

VI. Some Examples of Projected Motion

In this section we explicitly work out analytical expressions for $u(p, \theta, t)$ for two different image *sequences* and vector fields. We shall see that the resulting expressions are consistent with our previous findings and our intuitive expectations. We note that as the conservation assumptions underlying the integral PMI do not hold for either of these simple examples, the more general differential PMI is invoked throughout.

A. Example 1

Let $f(x, y, t) = \exp\left(-(x - v_1 t)^2 - (y - v_2 t)^2\right)$, and $v(x, y) = [x,\ y]^T$. See Figure 1. Computing the gradient of f we have

$$\nabla f = -2(1-t)^2 \exp\left(-(1-t)^2(x^2+y^2)\right)[x,\ y]^T. \tag{88}$$

Using properties **P4** and **P9** described earlier we get

$$\mathcal{R}_\theta\left[v^T \nabla f\right] = \mathcal{R}_\theta\left[-2(x^2+y^2)(1-t)^2 \exp\left(-(1-t)^2(x^2+y^2)\right)\right] \tag{89}$$

$$= \frac{-\sqrt{\pi}\exp\left(-p^2(1-t)^2\right)}{|1-t|}\left(2p^2(1-t)^2+1\right) \tag{90}$$

and

$$\frac{\partial g(p,\theta,t)}{\partial p} = \frac{\partial}{\partial p}\mathcal{R}_\theta[f] \tag{91}$$

$$= \frac{\partial}{\partial p}\frac{\sqrt{\pi}\exp\left(-p^2(1-t)^2\right)}{|1-t|} \tag{92}$$

$$= \frac{-2\sqrt{\pi}p(1-t)^2\exp\left(-p^2(1-t)^2\right)}{|1-t|}. \tag{93}$$

Invoking the differential PMI, and solving for u, we obtain

$$u(p,\theta,t) = p + \frac{1}{2p(1-t)^2}. \tag{94}$$

The above expression for u, which is independent of θ due to the rotational symmetry of the image and the isotropic nature of the motion field, displays a singularity at $t=1$. Upon close examination, we find this is not surprising since at $t=1$, $f(x,y,1)$ has null gradient and hence there is no perceived motion. Even with $t \neq 1$, there is still a singularity at $p=0$. The explanation for this is perhaps a bit more subtle. Namely, for $p = 0$, and regardless of the angle, all pixels in the image are moving in a perpendicular direction to $w(\theta)$. Hence, no motion can be measured in the projections.

More generally, considering affine motion as in (50); skipping the details of the computation, we obtain the *exact* expression

$$u(p, \theta, t) = v_0^T w + \frac{\operatorname{tr}(M) + \left(w^T M w\right)\left(2p^2(1-t)^2 - 1\right)}{2p(1-t)^2}, \tag{95}$$

which asymptotically agrees with our result in (83).

B. Example 2

To see the effect of rotational motion more explicitly, we choose $v(x, y) = [-y,\ x]^T$, and an image sequence f that is not rotationally symmetric: $f = [(x - v_1 t) + (y - v_2 t)] \exp\left(-(x - v_1 t)^2 - (y - v_2 t)^2\right)$. See Figure 2. The gradient of f turns out to be

$$\nabla f = \exp\left(-(1+t^2)(x^2+y^2)\right) \begin{bmatrix} -(t-1) - 2x(1+t^2)((t+1)y - (t-1)x) \\ (t+1) - 2y(1+t^2)((t+1)y - (t-1)x) \end{bmatrix}, \tag{96}$$

and

$$v^T \nabla f = ((t+1)x + (t-1)y) \exp\left(-(1+t^2)(x^2+y^2)\right). \tag{97}$$

Skipping the details, we obtain

$$u(p, \theta, t) = \frac{p\left[(t+1)\cos\theta + (t-1)\sin\theta\right]}{\left(1 - 2p^2(1+t^2)\right)\left[(t+1)\sin\theta - (t-1)\cos\theta\right]}. \tag{98}$$

The singularities in the above expression arise along the curve $2p^2(1+t^2) = 1$, and also when $(t-1)\cos\theta = (t+1)\sin\theta$. Away from the singular points, u vanishes for $p = 0$ regardless of the value of t and θ. This makes sense since the line integral of $v^T \nabla f$ shown in (97) is clearly zero over all lines going through the origin (i.e., $p = 0$ or $x = \alpha y$). Another way to say this is that over all such lines, the motion field and the gradient field are, *on average*, orthogonal. Hence, the net perceived motion in the projection, for $p = 0$, is zero.

We can further show that for any f defined in terms of Hermite polynomials as in (70) the expression for u resulting from rotation $v = [-y,\ x]^T$ becomes

$$u(p, \theta, 0) = \frac{\sum_{k,l} f_{kl} \cos^{k-1}(\theta) \sin^{l-1}(\theta) \left(k \sin^2(\theta) - l \cos^2(\theta)\right) H_{k+l}(p)}{\sum_{k,l} f_{kl} \cos^k(\theta) \sin^l(\theta) H_{k+l+1}(p)}, \tag{99}$$

which is consistent with (98) and behaves asymptotically as $1/p$ as we discussed in Section V.

VII. Relationship to Vector Tomography

One might wonder whether the study of motion from projections can be placed in the context of vector tomography. In a general vector tomography scenario, a vector field v is to be reconstructed from *inner product measurements* with respect to a probe $\mathbf{z}$ as follows:

$$g_{\mathbf{z}}(p,\theta) = \int\int \mathbf{z}(p,\theta)^T v(x,y)\delta(p - x\cos(\theta) - y\sin(\theta))\, dx\, dy. \tag{100}$$

The probe $\mathbf{z}(p,\theta)$ is itself a vector function which is *independent* of x and y. Comparing (100) to the right-hand side of the differential PMI (26), we can see that the vector "probe" in that case is actually the gradient of the image $f(x,y,t)$, which will, of course, depend upon x and y. On the other hand, for integral PMI (34), the probe is exactly the direction vector $w(\theta)$.

Two types of measurements are typically distinguished in vector tomography. The special case of $\mathbf{z}(p,\theta) = w(\theta)$ is referred to as a *transversal measurement*, whereas the case $\mathbf{z}(p,\theta) = w(\theta + \frac{\pi}{2})$, with the probe orthogonal to the p axis, is referred to as a *longitudinal measurement* [12], [13]. Helmholtz's Theorem [11] states that any vector field can be written as the sum of two components:

$$\begin{aligned} v(x,y) &= \nabla\phi(x,y) + \nabla \times (\psi(x,y)e_3) && (101)\\ &= v_I + v_S, && (102) \end{aligned}$$

where $\phi(x,y)$ and $\psi(x,y)$ are referred to as the scalar and vector potentials, respectively, and $e_3 = [0,\ 0,\ 1]^T$. The first term (v_I) on the right-hand side of (101) is referred to as the irrotational (or curl-free) component of v, whereas the second term (v_s) is the solenoidal (or divergence-free) component of v. Prince [12] has shown that any choice of the inner-product probe that satisfies $\mathbf{z}^T w \neq 0$ will reconstruct the irrotational part of v. In particular, this includes $\mathbf{z} = w(\theta)$. On the other hand, to reconstruct the solenoidal part of v, the choice of probe must be such that $\mathbf{z}$ is *not* parallel to $w(\theta)$; a convenient choice is the longitudinal probe $\mathbf{z} = w(\theta + \frac{\pi}{2})$. The end result is that the transversal probe $\mathbf{z} = w(\theta)$ determines the irrotational part of v, whereas the longitudinal probe $\mathbf{z} = w(\theta + \frac{\pi}{2})$ determines its solenoidal part.

As the probe $w(\theta)$ in the integral formulation of the PMI is purely transversal, it is only possible to reconstruct the irrotational part of the motion vector field v from measurements of u_c using existing techniques for vector tomography[5] [12], [13], [14]. On the other hand, the probe in the differential PMI formulation is the gradient of the image; and as such, it is neither purely transversal nor purely longitudinal in nature. Therefore, it appears that the measurements of u implied by the *differential* form of the PMI carry more information about the motion vector field than the corresponding values u_c implied by the integral PMI. As we saw earlier, however, for at least the class of images we studied, the effect of pure rotational motion in u dissipates as $1/p$ away from the image of the vortex (or the center of rotation) in the projection domain. It is therefore reasonable to argue that sufficiently far away from the vortex, the differential projected motion "probe" may essentially be considered transversal as well.

[5]Actually, the *flux* fv would be reconstructed first, and from this estimate, v could be recovered.

VIII. Conclusions and Future Directions

We considered the question of modeling the mapping between motion in an image (or image sequence) and its projections. To this end, we developed a local first order model (the differential Projected Motion Identity) and showed that it produces results that are reasonable and intuitive. We also studied alternative global formulations of the PMI based on conservation assumptions. In both cases, we derived several basic properties of projected motion. We studied the effect of affine motion in the projection domain using the differential formulation, particularly for a general class of images defined in terms of Hermite polynomials. This analysis revealed two interesting asymptotic phenomena in the projection domain. First, that the effect of pure rotation tends to be proportional to the inverse distance from the vortex in the projection domain, and is hence difficult to measure. Second, the effect of divergent and shearing motions were seen to be directly proportional to the radial distance away from the vortex.

More generally, the PMIs can be considered as indirect measurement equations for motion flow in the image domain. This implies an inverse problem. Namely, given measurements of the projections g and their respective motion field u (or u_c), how do we reconstruct v? We saw that the measurements u_c implied by integral PMI are transversal in nature and therefore yield information only about the irrotational component of v. Existing reconstruction algorithms [12], [13], [14] can be applied to recover the irrotational part of v from u_c. If v is purely solenoidal ($\text{div}(v) = 0$), however, the continuity equation (30) invoked in the derivation of integral PMI reduces to the familiar optical flow brightness constraint, and we see that u_c conveys *no* information about v in this case.

The more general case of inverting for v from measurements u implied by differential PMI seems to be an interesting and challenging inverse problem in its own right since these measurements contain some information about both solenoidal and irrotational components of the motion field v. Questions of existence and uniqueness of solutions, along with numerically well-behaved algorithms for performing the inversion remain to be studied. This inverse problem has a number of interesting applications. For instance, it has been shown [5], [6] that using (two) projections, we can efficiently estimate translational motion in the image. The natural next step would be to ask whether computationally efficient motion estimation algorithms using projections can be obtained for more general types of motion. As we saw in Section V, this seems to be possible in at least the affine case.

A solution to the inverse problem implied by the PMI is useful in any application where it may be difficult or impossible to collect inner product measurements of a vector field. In these cases, it may be possible instead to measure ordinary line integral projections of the density field, compute motion in these projections, and attempt to invert for the desired higher-dimensional vector field. This appears to be a promising direction of research that we will pursue in the future.

The concepts developed in this paper may be applied to a varied collection of practical problems. As we mentioned in the introduction, the correction of projection data that have been subjected to motion distortion is but one important application. Other application areas may include acoustic tomography, optical flow estimation and astronomy, to name a few.

References

[1] J.L.C. Sanz, E.B. Hinkle, and A.K. Jain, *Radon and projection transform-based computer vision*, Springer-Verlag, 1987.

[2] S. Alliney and C. Morandi, "Digital image registration using projections", *IEEE Trans. of Patt. Anal. Machine Intell.*, vol. PAMI-8, no. 2, pp. 222–233, March 1986.

[3] J.C. Wood and D.T. Barry, "Tomographic time-frequency analysis and its applications toward time-varying filtering and adaptive kernel design for multicomponent linear-fm signals", *IEEE Trans. on Sig. Proc.*, vol. 42, no. 8, pp. 2094–2104, July 1994.

[4] P. Milanfar, W.C. Karl, and A.S. Willsky, "A moment-based variational approach to tomographic reconstruction", *IEEE Trans. on Image Proc.*, vol. 5, no. 3, pp. 459–470, March 1996.

[5] Peyman Milanfar, "Projection-based, frequency-domain estimation of superimposed translational motions", *J. of the Opt. Soc. of Am.: A*, vol. 133, no. 11, pp. 2151–2161, November 1996.

[6] S. A. Rajala, A. M. Riddle, and W. E. Snyder, "Application of the one-dimensional Fourier transform for tracking moving objects in noisy environments", *Computer Vision, Graphics, and Image Processing*, vol. 21, pp. 280–293, February 1983.

[7] C. Crawford, K.F. King, C.J. Ritchie, and J.D. Godwin, "Respiratory compensation in projection imaging using a magnification and displacement model", *IEEE Trans. on Med. Imag.*, vol. 15, no. 3, pp. 327–332, June 1996.

[8] S.R. Deans, *The Radon transform and some of its applications*, Krieger, Malbar, FL, 1993.

[9] J.E. Marsden, *Elementary Classical Analysis*, W.H. Freeman and Company, 1974.

[10] J.M. Fitzpatrick, "The existence of geometrical density-image transformations corresponding to object motion", *Computer Vision, Graphics, and Image Processing*, vol. 44, pp. 155–174, 1988.

[11] P.M. Morse and H. Feschbach, *Methods of Theoretical Physics*, McGraw-Hill, New York, NY, 1953.

[12] Jerry L. Prince, "Tomographic reconstruction of 3-D vector fields using inner product probes", *IEEE Trans. on Image Proc.*, vol. 3, no. 2, pp. 216–219, March 1994.

[13] Hans Braun and Axel Hauck, "Tomographic reconstruction of vector fields", *IEEE Trans. on Sig. Proc.*, vol. 39, no. 2, pp. 464–471, February 1991.

[14] Stephen J. Norton, "Unique tomographic reconstruction of vector fields using boundary data", *IEEE Trans. on Image Proc.*, vol. 1, no. 3, pp. 406–412, July 1992.

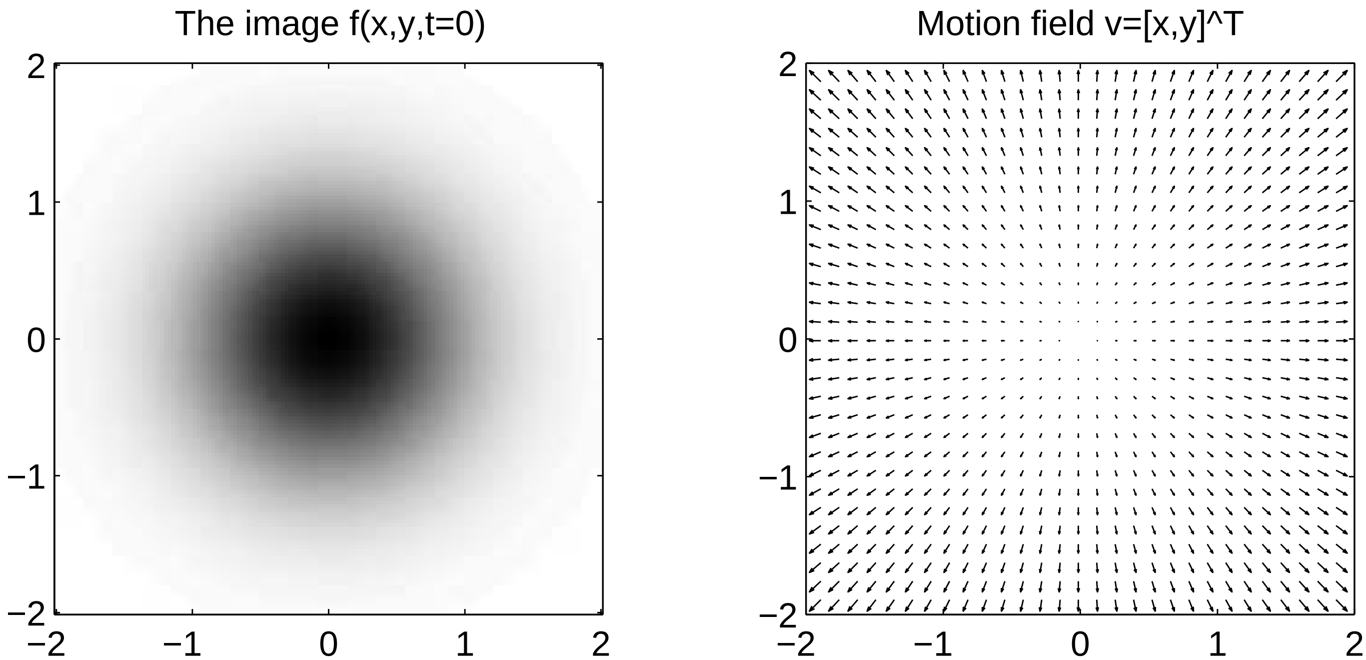

Fig. 1. The image f and the optical flow field for Example 1

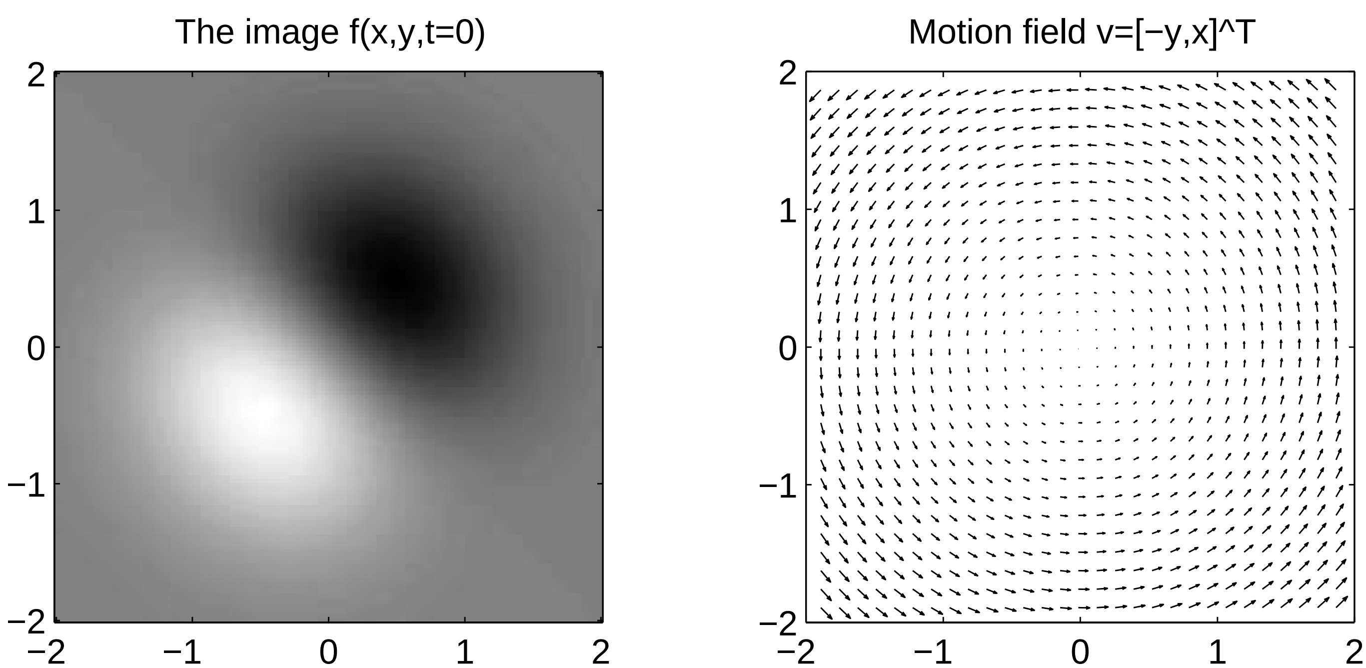

Fig. 2. The image f and the optical flow field for Example 2